Ocean Engineering 301 (2024) 117510

Contents lists available at ScienceDirect

Ocean Engineering

journal homepage: www.elsevier.com/locate/oceaneng

Research paper

Structural health monitoring on offshore jacket platforms using a novel ensemble deep learning model

Mengmeng Wang [a,b,c], Atilla Incecik [b], Zhe Tian [c,*], Mingyang Zhang [d], Pentti Kujala [e], Munish Gupta [f,g], Grzegorz Krolczyk [f], Zhixiong Li [c,f]

[a] College of Ocean Science and Engineering, Shandong University of Science and Technology, Qingdao, 266590, China
[b] Department of Naval Architecture, Ocean, and Marine Engineering, University of Strathclyde, Glasgow, G11XQ, United Kingdom
[c] Department of Marine Engineering, Ocean University of China, Qingdao, 266100, China
[d] Department of Mechanical Engineering, Marine Technology Group, Aalto University, Espoo, Finland
[e] Tallinn University of Technology, Estonian Maritime Academy, 19086, Tallinn, Estonia
[f] Faculty of Mechanical Engineering, Opole University of Technology, 45-758, Opole, Poland
[g] Department of Mechanical Engineering, Graphic Era Deemed to be University, Uttarakhand, 248002, India

ARTICLE INFO

Keywords:
Offshore jacket platform
Structural health monitoring
Deep learning
Damage detection

ABSTRACT

Monitoring health condition of offshore jacket platforms is crucial to prevent unexpected structural damages, where a prevailing challenge involves translating available feature information into structural damage patterns. Although the artificial neural network (ANN) models are popular in addressing this challenge, they often fail to capture the temporal correlations between the feature information and the damage patterns, which reduce their capability for discovering the laws governing the structural damage detection. To bridge this research gap, this study proposes a novel ensemble deep learning model to enhance the temporal feature extraction to improve the damage pattern identification. In this approach, a one-dimensional Convolutional Neural Network (CNN) extracts the spatiotemporal features from the structural vibration measurements. Simultaneously, a SENet attention mechanism is introduced to select the most informatic features. Subsequently, a bidirectional long short-term memory network (BiLSTM) is employed to learn the mapping between the extracted features and the structural damage patterns. Furthermore, the particle swarm optimization (PSO) algorithm is used to optimize the BiLSTM hyperparameters to enhance its stability and reliability. Both simulations and experiments are carried out to collect the vibration responses of the offshore jacket structure in different damage scenarios. The analysis results demonstrate that the proposed method produces remarkable improvement with respect to the accuracy and robustness in identifying the structural damages when compared with the ANNs. The overall detection accuracy of the proposed CNN-BiLSTM-Attention ensemble model is beyond 95%, which provides strong applicability to practical structural health monitoring of offshore platforms.

1. Introduction

Offshore jacket platforms are widely used in development and utilization of marine resources (Aeran et al., 2020; Asgarian et al., 2016; Zhang et al., 2022; Zhang et al., 2024). Each offshore jacket platform presents certain unique characteristics, such as high structural complexity, large dimensions, and intricate stress conditions. Due to be exposed to harsh marine environments (Xu et al., 2021), various types and degrees of damages, such as cracking, corrosion, deformation, and fractures, are often found on the offshore jacket platforms (D. Zhang et al., 2023). These damages can affect the stiffness, strength, stability, and durability of the offshore jacket platforms, and consequently, reduce the structure reliability and service life, as well as posing great risks of casualties and losses (Puruncajas et al., 2020). Therefore, it is critical to monitor the health condition of the offshore jacket platforms to ensure their safe operation and prolong their lifespan (Wang et al., 2022).

The damage pattern identification is essential in the health monitoring of the offshore jacket platforms. At present, traditional methods for damage identification can be classified into three categories, including the modal method based on vibration measurements (Asgarian et al., 2016; Huang et al., 2012; Xu et al., 2021), the ultrasonic method based on sound waves (Chen et al., 2022; Dou et al., 2022; Meng

* Corresponding author. Department of Marine Engineering, Ocean University of China, Qingdao, 266100, China.
E-mail address: tianzhe@ouc.edu.cn (Z. Tian).

https://doi.org/10.1016/j.oceaneng.2024.117510
Received 30 January 2024; Received in revised form 5 March 2024; Accepted 12 March 2024
Available online 21 March 2024

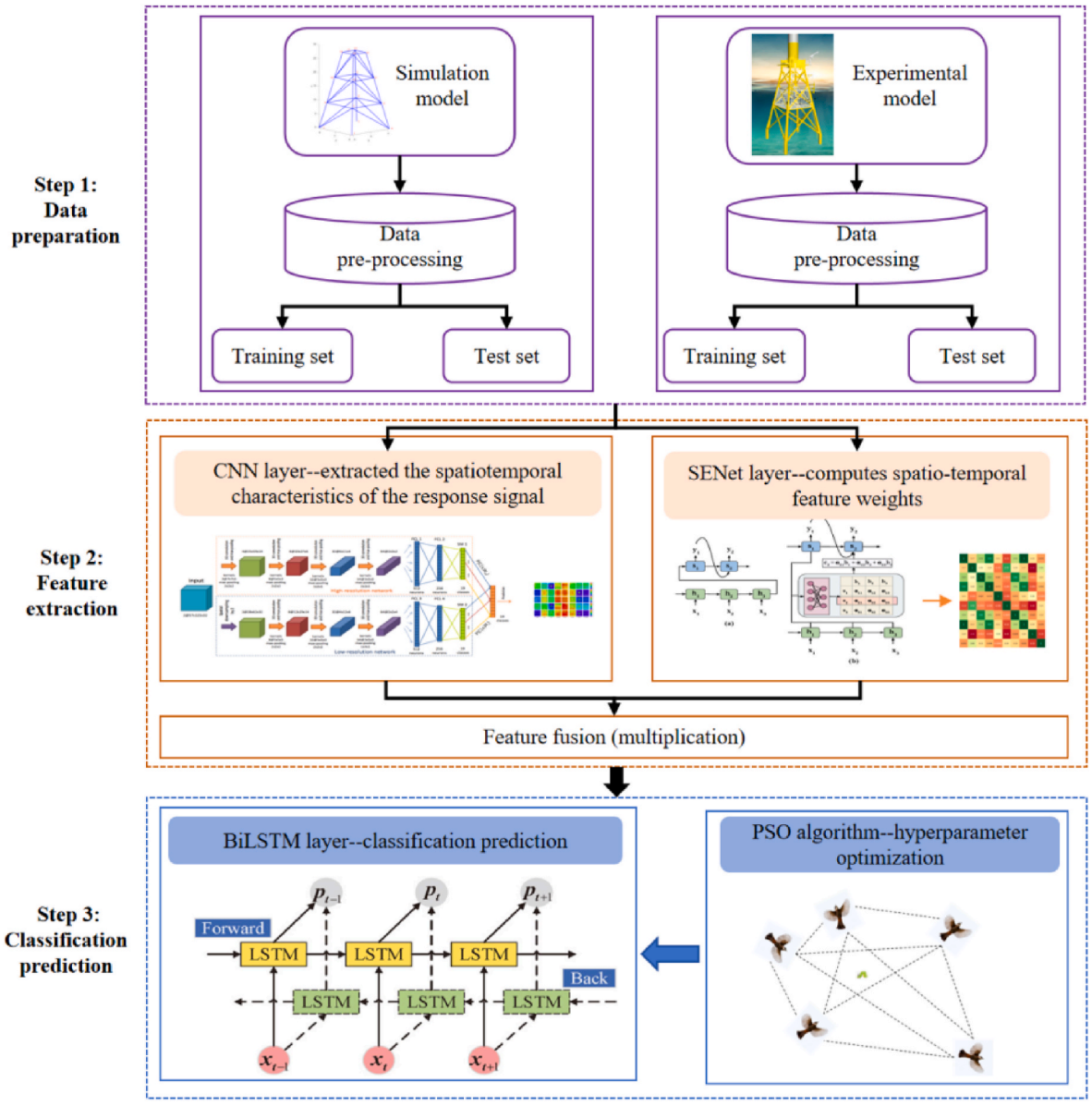

Fig. 1. The framework of the ensemble deep learning neural network.

et al., 2023; Qin et al., 2023), and the potential method based on electromagnetic fields (Guo et al., 2023; Lu et al., 2022; Ni et al., 2021; Zhang et al., 2022). The modal method utilizes the structural vibration characteristics (i.e., frequency, mode, and damping) to reflect changes in structural stiffness, strength, stability and other characteristics, thereby enabling the identification of the structural damages (Fathi et al., 2020). The advantages of the modal method include that it does not need to obtain data near the damage location and can identify underwater structural damages even if the vibration data are collected far away from the damage location; while the disadvantages are that its performance is greatly affected by the environmental noise and it is difficult to extract and identify modal parameters for complex jacket structures (Huang et al., 2012). The ultrasonic method utilizes the propagation characteristics of the sound waves in a medium to detect defects on the surface and inside the structures, such as cracks, corrosion, voids, etc. (Meng et al., 2023). This method can locate and quantify the subtle defects and is not limited by the shape and size of the structures; however, the ultrasonic usually requires clean and well-lubricated structure surfaces to drive the sound waves, and for underwater jacket structures, additional specially designed underwater probes and robots are required to perform the detection operations (F. Zhang et al., 2023). The potential method aims to detect the corrosion using the electromagnetic characteristics of the structures (Huang et al., 2022). The advantages of the potential method are that the overall corrosion can be quickly evaluated without physical contact and the detection process can be controlled remotely (Lu et al., 2022); while the disadvantages are that the structure needs cathodic protection to ensure the potential stability and the potential sensitivity is low for offshore structures (Zhang et al., 2022). From existing literature, it is noticed that although traditional methods have made great achievements in structural health monitoring, their disadvantages hinder their applications in marine structures due to harsh ocean environments (Mojtahedi et al., 2011).

Recently, the data-driven techniques based on artificial intelligence (AI) are popular for offshore structure monitoring (Balu et al., 2022; Cattaneo and Macchi, 2019; Chakraborty and Adhikari, 2021). By collecting the time series data of the structure dynamics (such as the acceleration, velocity, and displacement measurements), it is possible to use an ANN model to find useful damage features from the time series data to identify the damage patterns (Richmond et al., 2020). Generally, the data-driven techniques identify the damage patterns mainly through

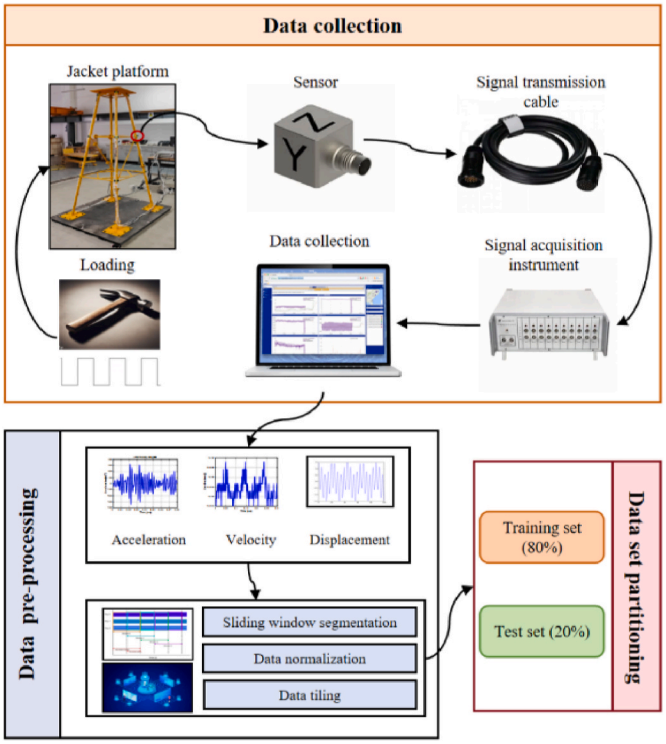

Fig. 2. Workflow of the data preparation step.

the model updating (Augustyn et al., 2020; Shiradhonkar and Shrikhande, 2011) or the pattern classification (Ghiasi et al., 2022; Jamshidi and El-Badry, 2023). The basic idea of the model updating regards the pattern identification as a classical optimization problem, which aims to reduce the inconsistency between the finite element (FE) model and the physic model of the offshore structure by updating the FE parameters using the measured time series data from the physic model (Khodaparast et al., 2011). Because the prior knowledge of the structure can be applied to the FE model, one can only choose necessary data sources from the time series for the model updating to reduce the computation complexity. However, for complex offshore structures, it is often difficult to update the FE parameters due to a large number of structure parameters (Mojtahedi et al., 2020). To address this issue, the pattern classification method is introduced by using the machine learning to extract useful damage features directly from the time series without establishing an FE model. Typical machine learning models include the CNN (Moradzadeh et al., 2022; Pan et al., 2023; Wang et al., 2023), XGBoost (Ahmadian et al., 2024), Dictionary Learning (DL) (Mousavi et al., 2023), Extreme Learning Machine (ELM) (Utaminingrum et al., 2023), Support Vector Machines (SVM) (Kouchaki et al., 2023), and Radial Basis Function (RBF) (Zahs et al., 2023). However, most existing machine learning models encounter difficulties in gradient disappearance and gradient explosion when processing time series data, which may result in model overfitting or underfitting problems (Ebrahimian et al., 2017; Fathi et al., 2020; Liu et al., 2018). In addition, due to a large number of features that can be extracted by the machine learning from the jacket structure dynamics, it is difficult to determine/select the most informatic features while remove the useless/redundant ones. Although the CNN is more powerful than most existing machine learning models in feature extraction (Pan et al., 2023) because it can keep the spatiotemporal characteristics of the data, each extracted feature is treated equal-importantly without any feature selection processing; as a result, the damage pattern identification will be influenced if inappropriate features are adopted (Bao et al., 2021). Therefore, it is crucial to address these issues for the health monitoring of offshore structures (Moradzadeh et al., 2022; Pan et al., 2023).

To address the research gap in data-driven offshore structure monitoring, this study proposes a novel ensemble deep learning model (named as CNN-BiLSTM-Attention model) to overcome the challenge in the damage feature selection to improve the structural damage recognition. In this new model, a SENet attention mechanism is integrated with a one-dimensional CNN to evaluate the importance of the CNN-extracted features and select the damage-sensitive features. Then, a BiLSTM network is built to learn the mapping between the features and structural damage patterns; to avoid model overfitting/underfitting, the PSO is used to optimize the BiLSTM hyperparameters. Experimental evaluation results indicate significant improvement on the structural damage identification using the proposed method.

This paper is organized as follows: Section 2 introduces the proposed method; In Section 3 and Section 4, FE simulation and experimental evaluation are respectively performed to verify the validity of the proposed method. Section 5 draws the conclusions.

2. Methodology

To improve the identification of damage patterns, an ensemble deep learning model that combines CNN, BiLSTM, and an attention neural network is proposed for offshore structure health monitoring. Fig. 1 provides an overview of the proposed ensemble method.

The implementations of the proposed ensemble model are described as follows.

(a) Firstly, the one-dimensional CNN is employed to extract the time series features from structural vibration responses;
(b) And then, a SENet (squeeze-and-excitation networks)-based attention mechanism is incorporated into the CNN layers to evaluate the feature importance, so as that the most informatic features will be selected by assigning large weight values while the useless/redundant features can be removed by assigning small weight values.
(c) Lastly, a BiLSTM model is used to exploit the optimized features to establish the identification map between the features and damage patterns.
(d) During the BiLSTM learning process, the PSO is employed to optimize the BiLSTM hyperparameters to reduce the tedious process of parameter tuning.

The rationale behind selecting this ensemble model over other potential architectures is elaborated as follows.

First of all, the CNN are renowned for its exceptional ability to extract features from images and sequence data (Kilic et al., 2023). Existing literature suggests that the CNN is more powerful than other popular machine learning models in feature extraction (Pan et al., 2023). Hence, it is reasonable to incorporate the CNN into the proposed ensemble model with the purpose that key features associated with the structural damages can be extracted as a solid foundation for the damage pattern recognition. Considering that the one-dimensional CNN is designed to process time series data (Serkan et al., 2021), it is reasonable to select it as the feature extraction method in the proposed model.

Secondly, the attention mechanism is widely used to evaluate essential aspects of the input data by amplifying critical details. More importantly, it is seamless to adopt the attention mechanism in the CNN architecture (Wang et al., 2023). In this study, the attention mechanism allows the CNN to concentrate on these features that significantly impact the recognition outcomes, thereby to improve the structural damage identification.

Thirdly, the BiLSTM demonstrate superior performance in handling time-series data ((Aravind Britto et al., 2023)). Because the BiLSTM is capable of capturing long-term dependencies within the data, it is suitable to use the BiLSTM to process the time series measurements of the offshore platform vibration.

As a result, the ensemble model aggregates several machine learning

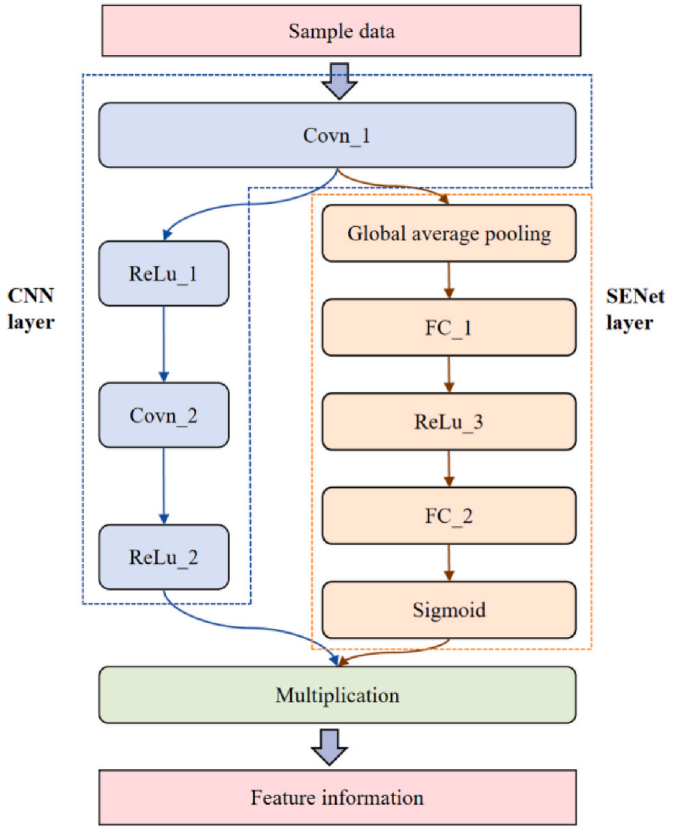

Fig. 3. The flowchart of the feature extraction.

algorithms with their unique advantages to enhance the performance of the damage pattern classification for offshore platforms.

2.1. Step 1: data preparation

In this step, the vibration measurements of the offshore structure are collected through FE simulations and prototype experiments in different health conditions. Then the data preprocessing is conducted, including the data segmentation, data normalization, and data tiling, to improve the quality and usability of the collected vibration data. The processed data are divided into the training set and test set for respectively training and testing of the ensemble model. The detailed flowchart of the data preparation is shown in Fig. 2.

Simulation and experimentation are two main tools for data preparation. In the simulation, the FE model of the offshore jacket platform is established to simulate different damage conditions by setting the elastic modulus of the defected elements based on the structure dynamics. In the simulation experiment, a prototype of the offshore jacket platform is developed and the structural damages are imposed on the prototype by reducing the cross-sectional areas of the defected elements. A vibrator and the pulse load are applied to the prototype to simulate the wave, wind, and current forces in the ocean environment. The vibration sensors such as accelerometers and displacement transducers are installed at the key nodes of the prototype to collect the structure vibration

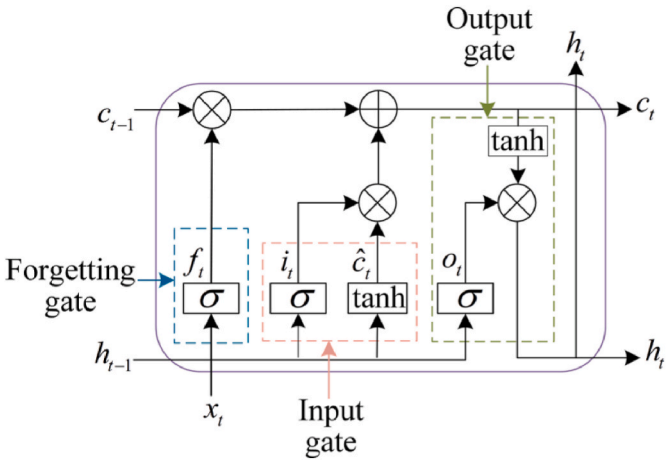

Fig. 5. A single LSTM model.

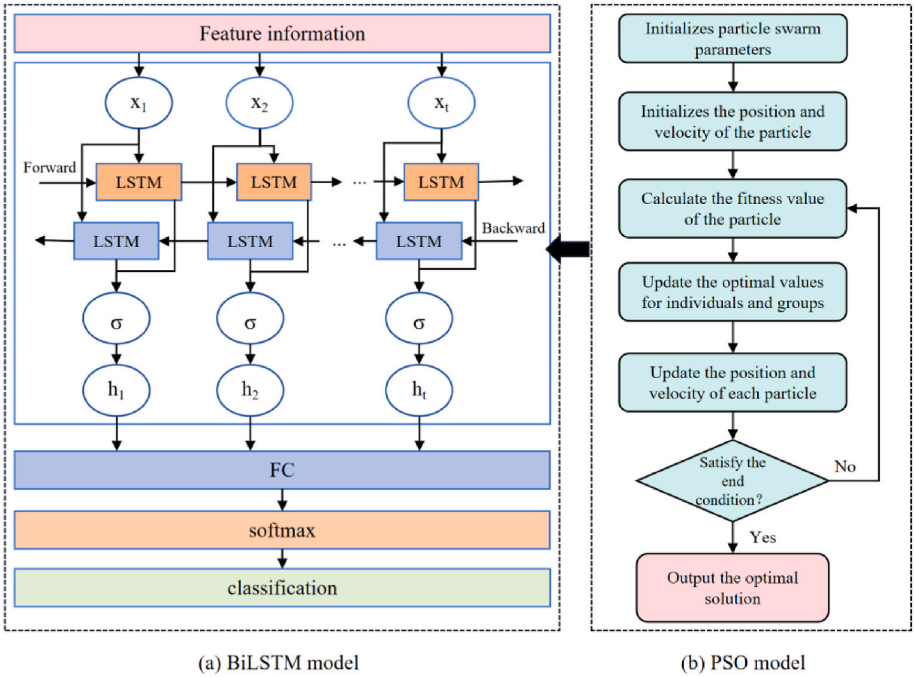

(a) BiLSTM model (b) PSO model

Fig. 4. The flowchart of the damage pattern identification.

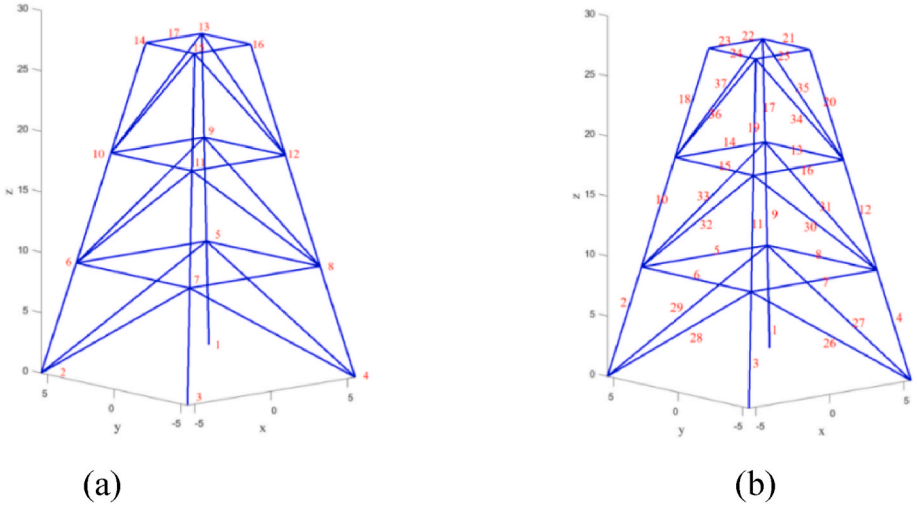

Fig. 6. The FE model: (a) the node representation, and (b) the element numbers.

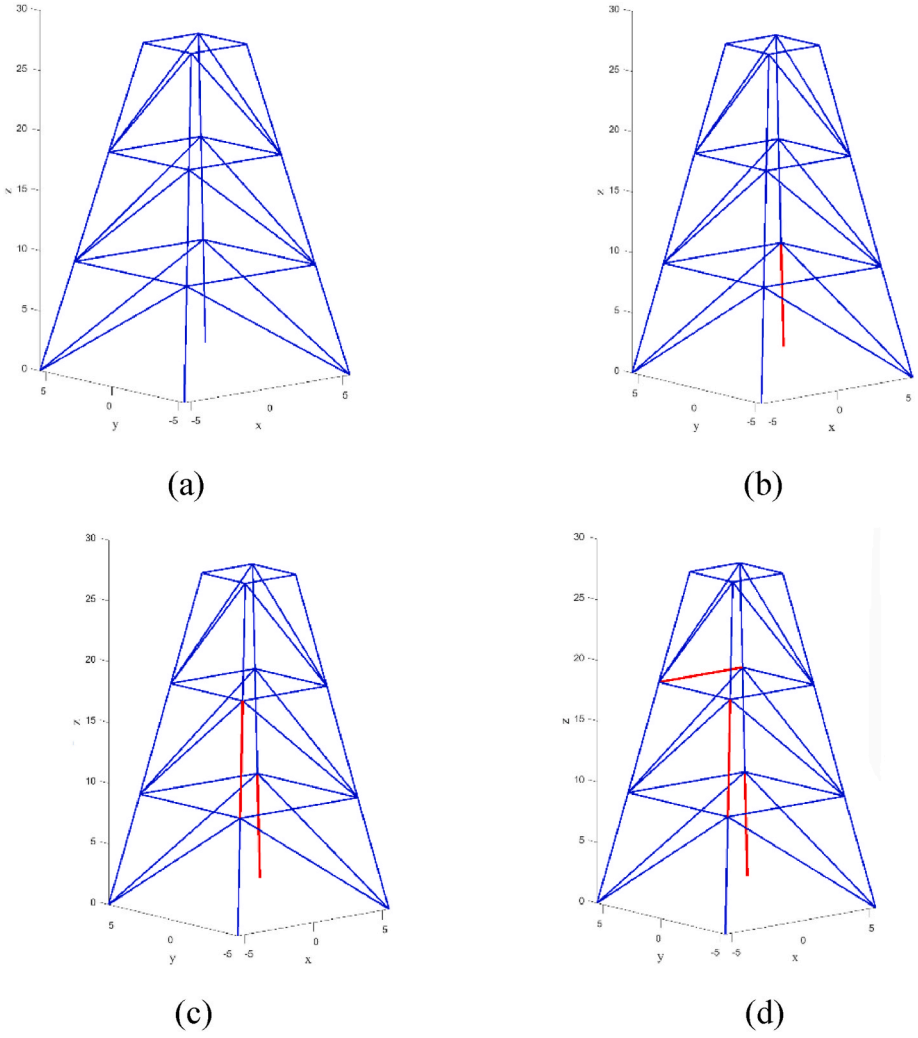

Fig. 7. Damage scenarios. (a) Normal condition; (b) single damage model; (c) double damage model; (d) multiple damage model.

responses. The collected data are transmitted to the computer through a signal transmission module for data storage and preprocessing.

In the data preprocessing, the vibration data is segmented by the overlapping segmentation method (Nguyen et al., 2015). Then, the data are normalized using the Min-Max normalization operation according to Eq. (1).

Table 1
Simulation conditions.

Health condition	Damage location	Damage degree
Normal	0	0
Single-damage	Element no. 1	50%
Double-damage	Element no. 1 and	70%, 50%
Multiple-damage	Element no. 1, 11 and 14	70%, 50%, 50%

$$x^* = \frac{x - min}{max - min} \tag{1}$$

where x is the original data, x^* denotes the normalized data, min and max respectively denote the minimum and maximum values in the original data. The normalization ensures the scale consistency of the data and improves the fitting effectiveness of the deep learning model. Then, the normalized data is tiled to ensure that each segment of the data is sequentially spliced into a one-dimensional vector to conform to the one-dimensional CNN.

2.2. Step 2: feature extraction

Fig. 3 illustrates the flowchart of the feature extraction step, including the feature extraction by the CNN and the feature selection by the SENet attention mechanism.

Firstly, the vibration data is fed through the first convolutional layer (covn_1) of the CNN model to perform the convolution operation to generate the first-layer features. The ReLU is used as the activation function. The mathematical expression for the convolutional layer is

$$x_j^l = f\left(\sum_{i \in M_j} x_i^{l-1} * \omega_{ij}^l + b_j^l\right) \tag{2}$$

$$ReLU(x) = max(0, x) \tag{3}$$

where x_j^l is the output of the jth channel of the l layer; x_j^{l-1} is the output of the jth channel of the l-1 layer; i and j denote the positional information of the convolutional filter; ω_{ij}^l denotes the weight of the convolutional kernel and b_j^l denotes the bias of the convolutional kernel; $f(.)$ is the activation function; and M_j denotes the feature map in the jth channel.

Then the first-layer features are input into the second covn_2 convolutional layer to reduce the feature size to generate the second-layer features; and two activation functions ReLU_1 and ReLU_2 are used to rectify the obtained features.

In parallel, the SENet attention mechanism is activated after the convolution layer (Conv_1). The attention mechanism adaptively evaluates the importance of each feature channel and assigns an appropriate weight to each one. By doing so, the important features will be enhanced while the unimportant ones will be suppressed using the weights. The procedure of the SENet attention mechanism is described as follows.

(a) Firstly, the output features of each convolution layer undergo a global average pooling operation to produce channel-wise statistical features;
(b) Two fully connected layers (a reduction layer and an excitation layer) are used to evaluate the channel-wise statistical features;

Table 2
The parameters of ensemble deep learning neural network.

Parameter	Value
Batch_size (size of the batch)	200
Filters (number of convolution cores)	6
Epochs (iteration number)	800
The channel of covn_1	32
The channel of covn_2	64
Optimizer	Adam

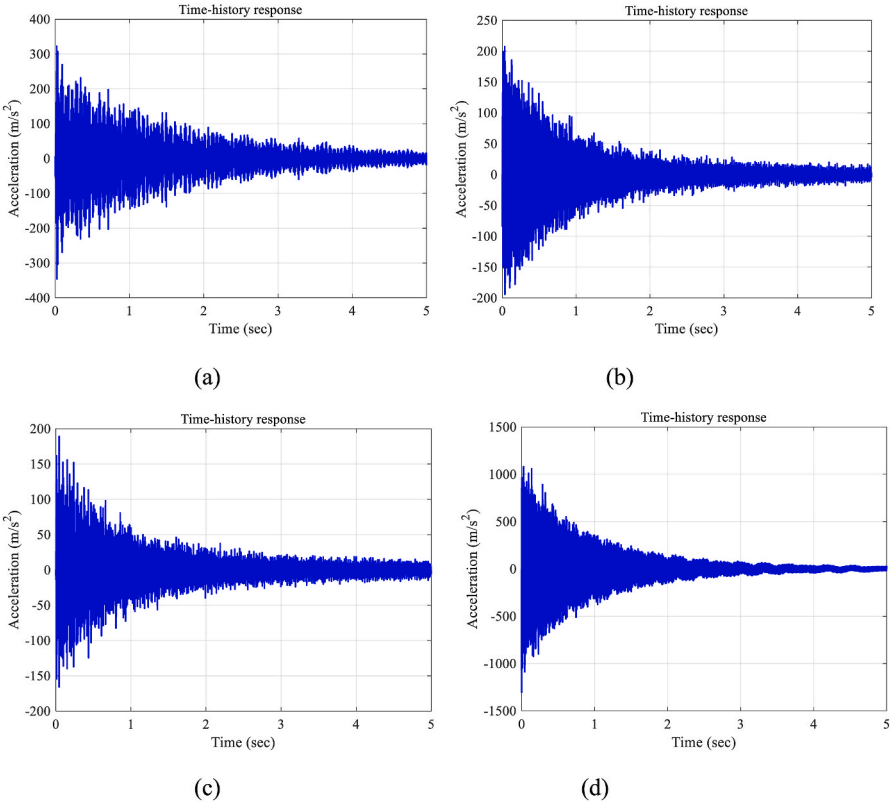

Fig. 8. Vibration responses of the FE model at degrees of freedom of (a) 52; (b) 60; (c) 72; (d) 84.

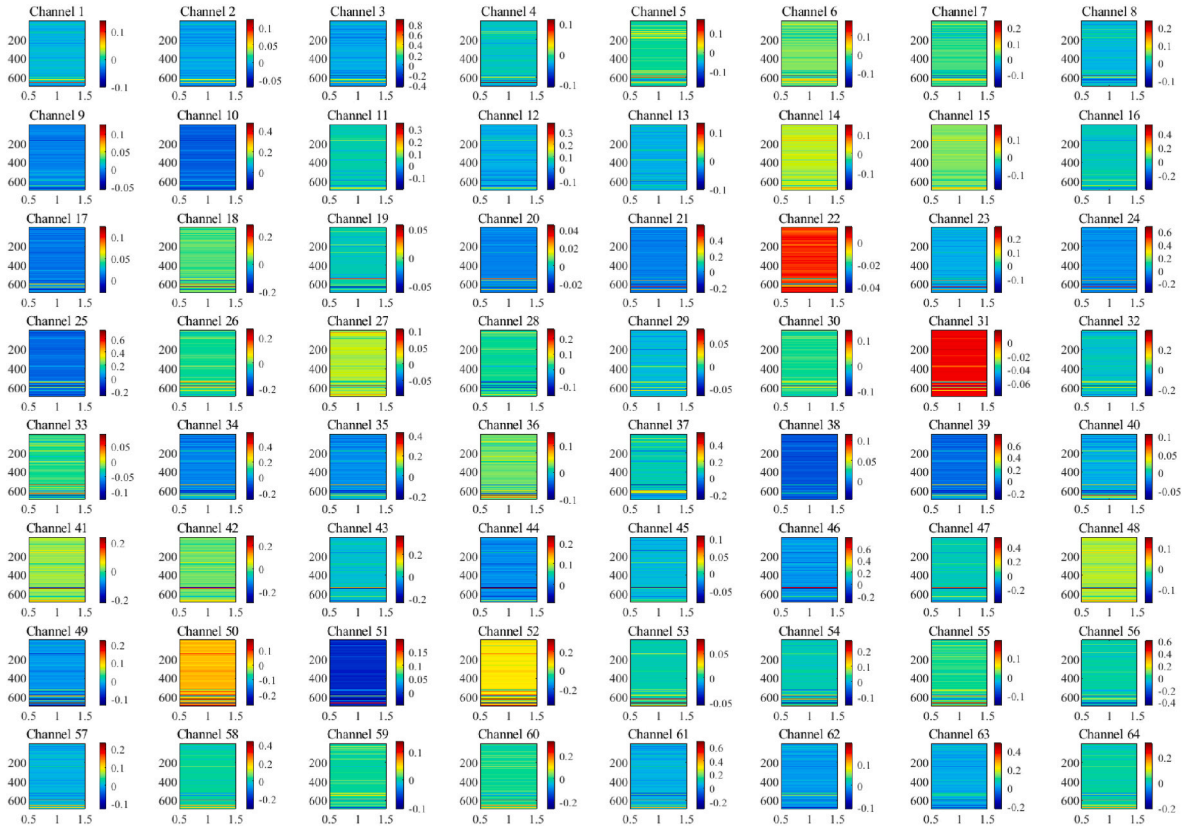

Fig. 9. Second-layer feature map of the CNN extraction.

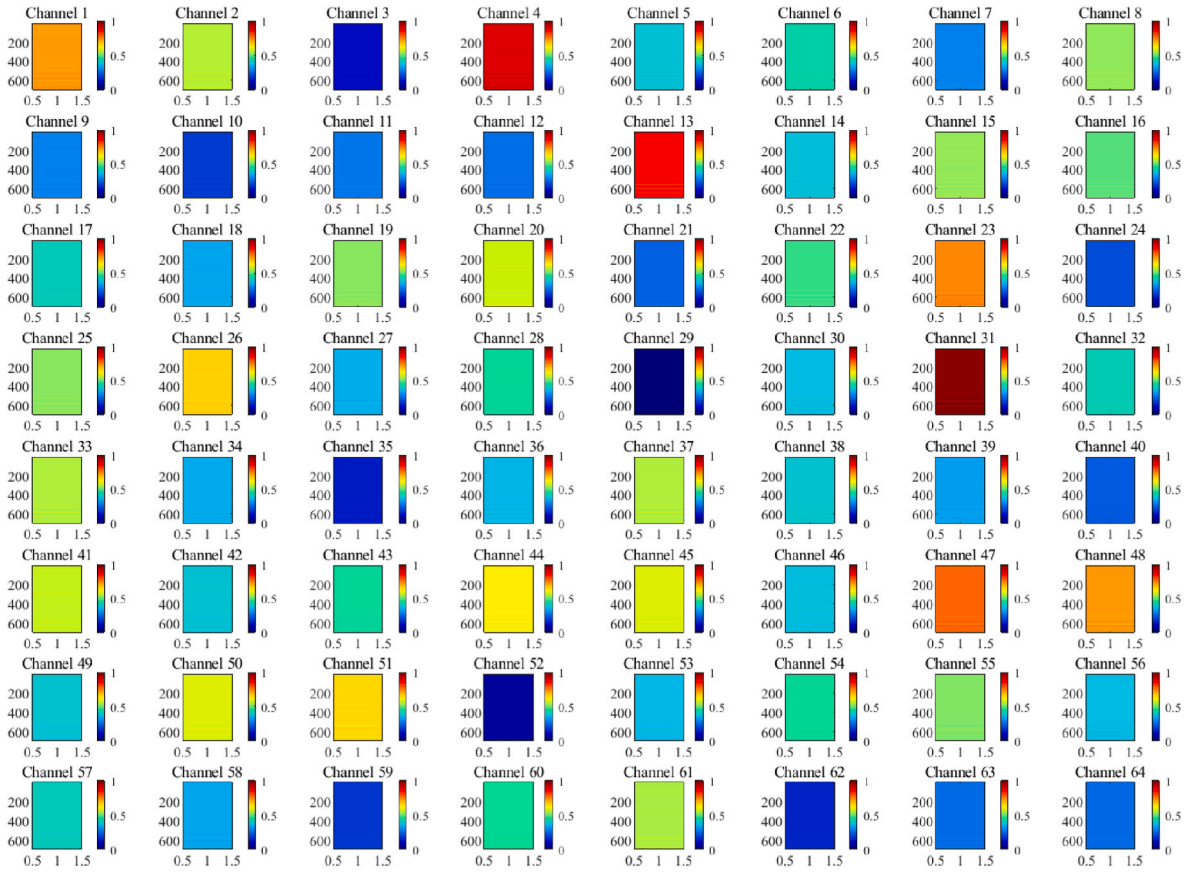

Fig. 10. The calculated weight by the SENet attention mechanism.

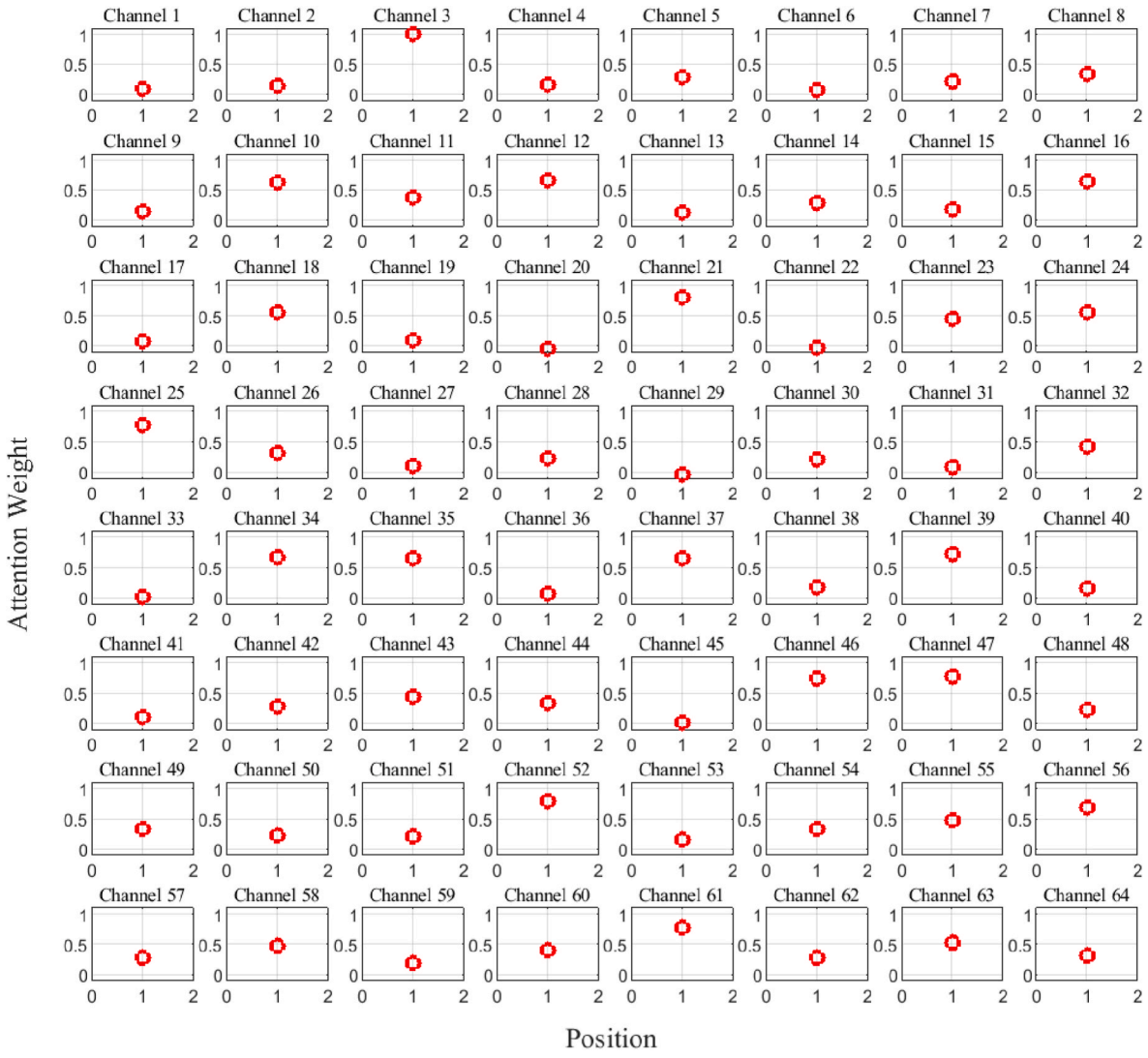

Fig. 11. The weight information of each feature channel in the conv_2 convolution layer.

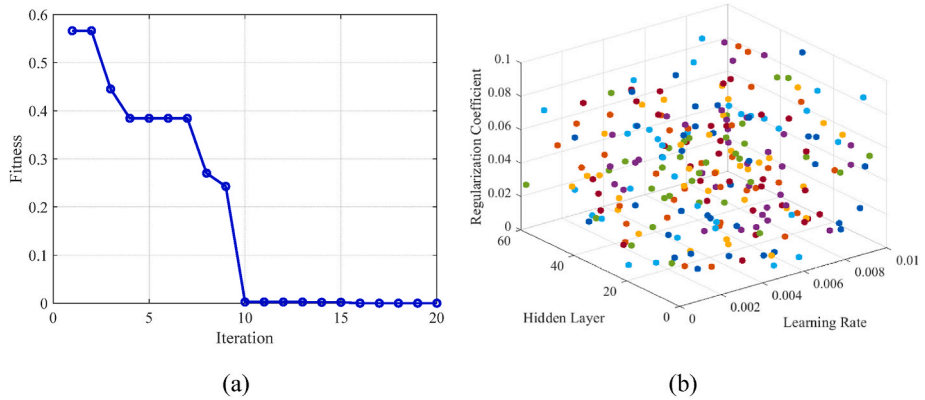

Fig. 12. PSO optimization results. (a) The changes of the fitness function; (b) Particle distribution.

(c) A sigmoid activation function is employed to produce the weight for each feature channel.

The nonlinear interaction between different feature channels is captured by two fully connected layers FC_1 and FC_2, and the weight values of each feature channel is calculated according to Eq. (4).

$$s = F_{ex}(z, W) = \sigma(g(z, W)) = \sigma(W_2\delta(W_1 z)) \tag{4}$$

where s is the channel weight; $\delta()$ is the activation function for dimensionality reduction of the input data z; W_1 and W_2 are the weight coefficients; $\sigma()$ is the sigmoid function, which restores z to its original dimensions.

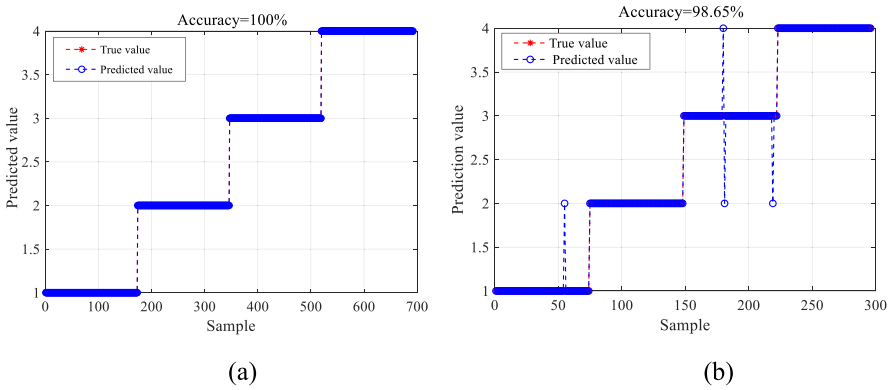

Fig. 13. Damage pattern identification results: (a) training set; (b) testing set.

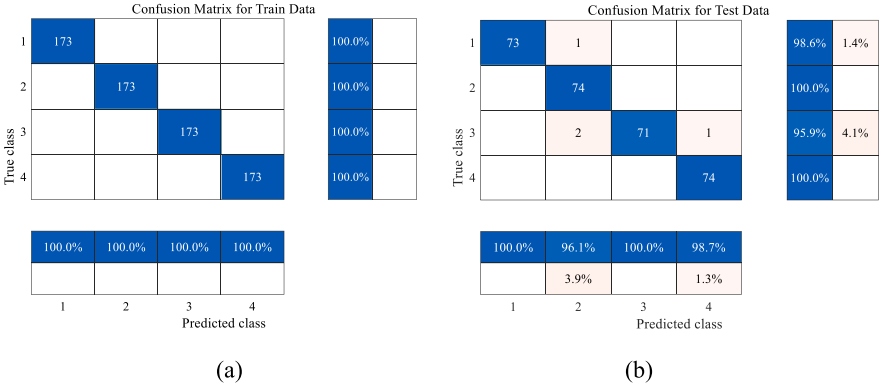

Fig. 14. Confusion matrix for damage pattern identification: (a) training set; (b) testing set.

Table 3
The comparison of results of different algorithms.

Model	*Accuracy*	*Precision*	*Recall*	*F*1 score
CNN	0.4696	0.4855	0.4696	0.4774
BiLSTM	0.9324	0.9353	0.9324	0.9339
CNN-BiLSTM-Attention	0.9865	0.9870	0.9863	0.9867

A very small weight value will be assigned to a useless feature channel while a large weight value will be assigned to an informatic feature channel at the multiplication layer. The feature weights are recalibrated according to Eq. (5) to select the most useful features.

$$\widetilde{x_c} = F_{scale}(u_c, s_c) = s_c u_c \tag{5}$$

where $\widetilde{x_c}$ is the output of the multiplication layer, s_c is the weight calculated by the SENet layer, and u_c is the feature extracted by the CNN.

Through the attention mechanism, useless/redundant features can be eliminated by assigning zero weights to them. This adaptive feature readjustment allows the CNN to focus on the information most relevant to the task to complete the feature selection.

2.3. Step 3: damage pattern identification

In the third step, a BiLSTM model is established to classify the damage patterns of the jacket structure. To avoid cumbersome trial-test parameters tuning, the PSO is used to optimize the hyperparameters of the BiLSTM model. The detailed damage identification implementation is shown in Fig. 4.

In this study, the number of hidden layers, learning rate and regularization coefficient of the BiLSTM are considered as critical hyper-parameters to be optimized. The PSO is adopted for this task. Assuming that there are N particles in a D-dimensional search space, the position X_{id} and velocity V_{id} information of the ith particle can be expressed as

$$X_{id} = (x_{i1}, x_{i2}, ..., x_{iD}) \tag{9}$$

$$V_{id} = (v_{i1}, v_{i2}, ...v_{iD}) \tag{10}$$

$$P_{id,best} = (p_{i1}, p_{i2}, ..., p_{iD}) \tag{11}$$

$$P_{d,gbest} = \left(p_{1,gbest}, v_{2,gbest}, ...v_{D,gbest}\right) \tag{12}$$

where $P_{id,best}$ is the optimal position of the *ith* particle and $P_{d,gest}$ is the group optimal position. The speed and position of each particle are updated according to Eqs. (13) and (14) to determine the distance and direction in the next movement (Karthika and Rathika, 2024).

$$v_{id}^{k+1} = \omega v_{id}^{k} + c_1 r_1 \left(p_{id,pbest}^{k} - x_{id}^{k}\right) + c_2 r_2 \left(p_{d,gbest}^{k} - x_{id}^{k}\right) \tag{13}$$

$$x_{id}^{k+1} = x_{id}^{k} + v_{id}^{k+1} \tag{14}$$

where ω is the inertia weight; c_1 is the individual learning factor; c_2 is the group learning factor; r_1 and r_2 are random number generated between [0, 1] to increase the randomness of search; v_{id}^{k} represents the d dimensional velocity of particle i in the k iteration; x_{id}^{k} represents the d dimensional position vector of particle i in the k iteration; $p_{id,pbest}^{k}$ represents the d dimensional historical optimal position of particle i in the k iteration; $p_{d,gbest}^{k}$ represents the d dimensional historical optimal position of the population in the k iteration, that is, the optimal solution in the entire population. When the PSO reaches the convergence

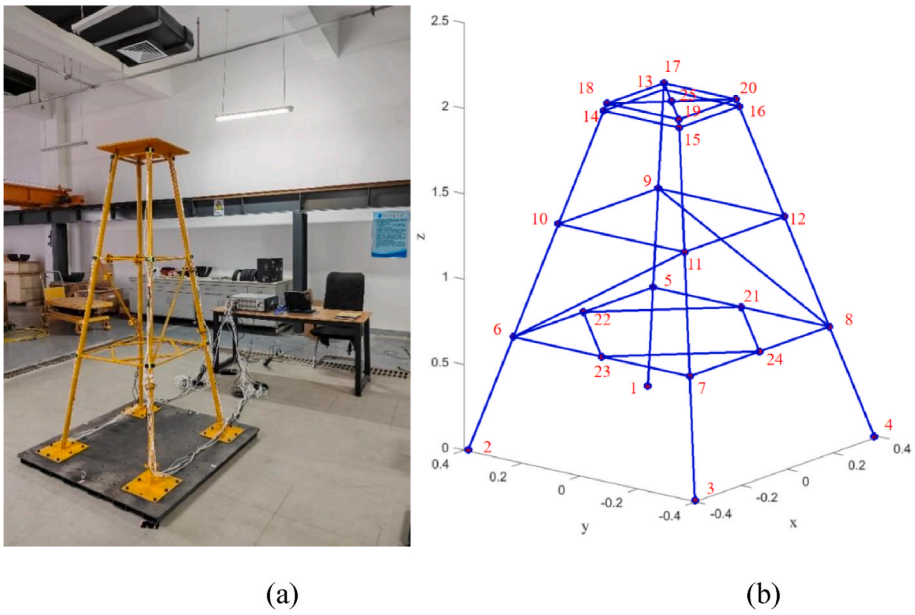

Fig. 15. Prototype of the jacket platform. (a) An image; (b) the node representation.

Table 4
Damage setting in the prototype.

Condition	Damage location	Outside diameter of replace rod
Normal	–	–
Single-damage	Element no. 10	21 mm
Double-damage	Element no. 10 and 8	21 mm and 21 mm
Multiple-damage	Element no. 10, 8 and 41	21 mm, 21 mm, and 10 mm

condition or the number of iteration steps, the optimization terminates.

Then, the optimized hyper parameters are substituted into the BiLSTM model for the damage pattern classification. The BiLSTM consists of two LSTM layers, including the forward LSTM and the reverse LSTM. The schematic diagram of a single LSTM is shown in Fig. 5.

As can be seen from Fig. 5 that the basic structure of the LSTM includes the input gate, forgetting gate and output gate, which work together to control the information flow and update the LSTM.

The forgetting gate selectively forgets the information unrelated to the current state and retains useful information in the memory cell state. Through a sigmoid function, the forgetting gate checks each state value and outputs numbers between 0 and 1, where 0 means "completely forget" and 1 means "completely retain". The relationship between the output of the previous moment and the input of the current moment can be expressed as:

$$f_t = \sigma\left(W_f \cdot [h_{t-1}, x_t] + b_f\right) \tag{15}$$

where $\sigma()$ is the sigmoid activation function; W_f is the weight; b_f is bias; h_{t-1} is the output of the previous moment; x_t is the input of the current moment.

The input gate decides how much of the new incoming information should be added to the cell state. This is achieved through a sigmoid function and a tanh function, where the former decides which values will be updated, and the latter creates a new candidate vector. The information is updated as

$$i_t = \sigma(W_i \cdot [h_{t-1}, x_t] + b_i) \tag{16}$$

$$\widehat{c}_t = tanh(W_c \cdot [h_{t-1}, x_t] + b_c) \tag{17}$$

$$c_t = c_{t-1} \cdot f_t + \widehat{c}_t \cdot t_t \tag{18}$$

where c_t is the current status information; W_i and W_c are the weight coefficients; b_i and b_c are the bias constant.

The output gate controls which part of the cell state should be output to the next layer using a sigmoid function; and then, the cell state passes through a tanh function (to keep input values between −1 and 1) and multiplies with the output of the sigmoid function to retain the selected information of the output gate. The current information of the output gate is

$$o_t = \sigma(W_o \cdot [h_{t-1}, x_t] + b_o) \tag{19}$$

$$h_t = o_t \cdot tanh(c_t) \tag{20}$$

where h_t represents the output at the current time and b_o is the bias constant.

In the classification process, the coordinated work of these three gates allows the LSTM to effectively remember long-term information while ignoring irrelevant data, which is particularly important for the time-series data processing (Aravind Britto et al., 2023). The three gates in the LSTM structure perform operations such as matrix multiplication and nonlinear summation in the memory cell to ensure that their memory does not decay during computational iterations. By maintaining and updating the cell state, the LSTM is able to retain memory of previous information, thereby making more accurate classification.

In the BiLSTM model, the forward LSTM is used to analyze the past state of the input data, and the reverse LSTM is used to analyze the future state of the input data. The forward LSTM and reverse LSTM are described by Eqs. (21)–(23).

$$\overrightarrow{h_t} = \overrightarrow{LSTM}(h_{t-1}, x_t, C_{t-1}), \quad t \in [1, T] \tag{21}$$

$$\overleftarrow{h_t} = \overleftarrow{LSTM}(h_{t+1}, x_t, C_{t+1}), t \in [T, 1] \tag{22}$$

$$H_t = \left[\overrightarrow{h_t}, \overleftarrow{h_t}\right] \tag{23}$$

where T represents the length of the time series and h_t represents the output at the current time. The full connection layer and the softmax activation layer are used to perform the classification task by generating the probability distribution of the class information.

To comprehensively evaluate the performance of the proposed ensemble model, the *Accuracy, Precision, Recall* and *F*1 score are taken as

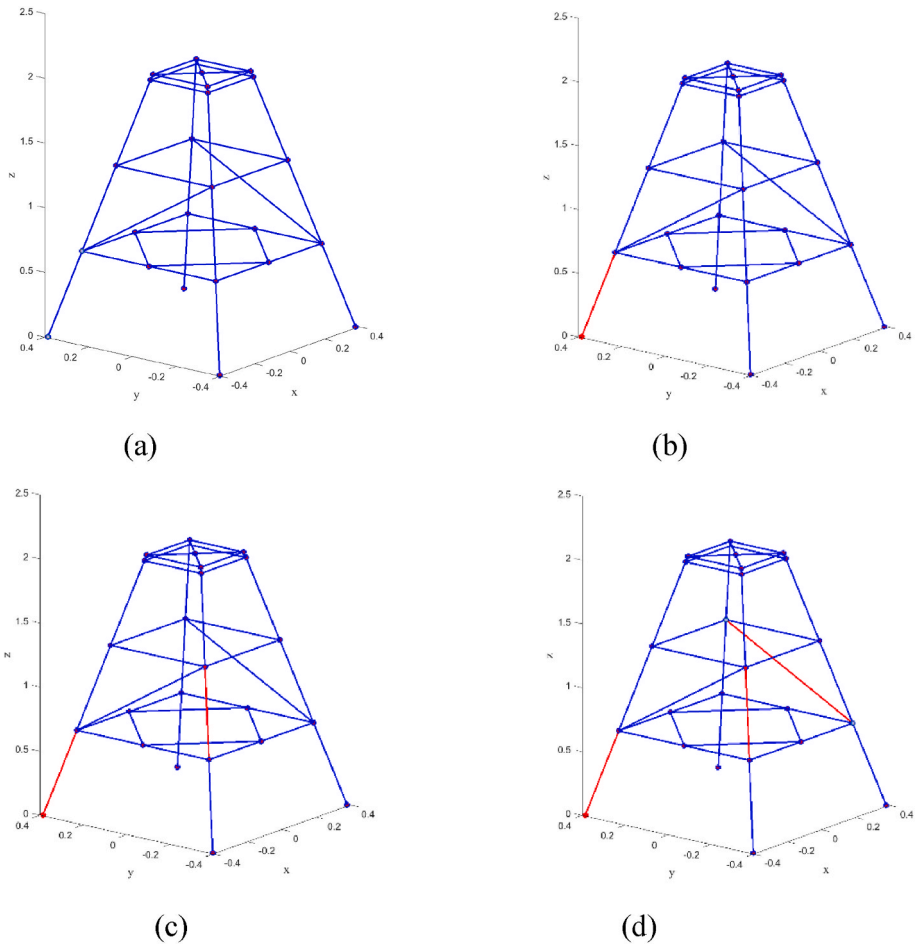

Fig. 16. Four health conditions in the experiments: (a) normal condition; (b) single-damage condition; (c) double-damage condition; (d) multiple-damage condition.

the evaluating indexes. The calculation formula are expressed as (Aravind Britto et al., 2023)

$$Precision = \frac{TN}{TN + FP} \tag{24}$$

$$Recall = \frac{TN}{TN + FN} \tag{25}$$

$$F1 = \frac{2{*}Recall{*}Precision}{Recall + Precision} \tag{26}$$

$$Accuracy = \frac{TP + TN}{TP + TN + FN + FP} \tag{27}$$

where *TP* is the true positive, *TN* is the true negative, *FP* is the false positive, and *FN* is the false negative.

The *Accuracy* is the most intuitive performance metric, reflecting the overall ability of the ensemble model to correctly identify the damage patterns. A high *Accuracy* rate means that the ensemble model is promising in distinguishing the damaged and undamaged structure patterns, which is crucial for structural health monitoring. *Precision* measures the proportion of the correctly identified damage patterns. A high *Precision* rate reduces the possibility of false positives, i.e., non-damaged structures being wrongly marked as damage patterns, which helps avoid unnecessary inspections and maintenance. *Recall,* also known as sensitivity, measures the proportion of correctly identified damage patterns to the total actual damage patterns. A high *Recall* rate means that the model can capture more true damage situations to reduce missed detections. *F*1 score is the harmonic mean of the *Precision* and *Recall*, aiming to balance the impact of the *Precision* and *Recall*. A high *F*1 score means that while maintaining precise damage identification, the ensemble model can also capture most of the true damage patterns. The *F*1 score is an important indicator to characterize the overall performance of the ensemble model. Combining these four metrics provides a comprehensive perspective to evaluate the efficacy of the ensemble model in identifying the damages of the offshore jacket structures.

3. FEM simulations

3.1. FE modelling

A FE model of the offshore jacket structure is established to perform simulations of the structure in different health conditions. The details of the FE model are described in Wang et al. (2023). The node number and element number of the FE model are illustrated in Fig. 6.

The loss of elastic modulus of the element of interest in the FE model is used to simulate the structure damage. Four health conditions were simulated in this study, including the normal FE model condition, single-damage FE model, double-damage FE model and multiple-damage FE model, as shown in Fig. 7. Detailed damage conditions are listed in Table 1.

The vibration responses of the FE model in different health conditions were collected with a sample frequency of 1000 Hz. Fig. 8 depicts the vibration responses of the FE model with 52, 60, 72, and 84 degrees of freedom in the normal health condition.

It is observed from Fig. 8 that all the vibration waveforms present a convergence trend in amplitude. This phenomenon can be attributed to the damping effect of the structure. Based on the vibration measurements in Fig. 8, the sliding window technique was used to segment the

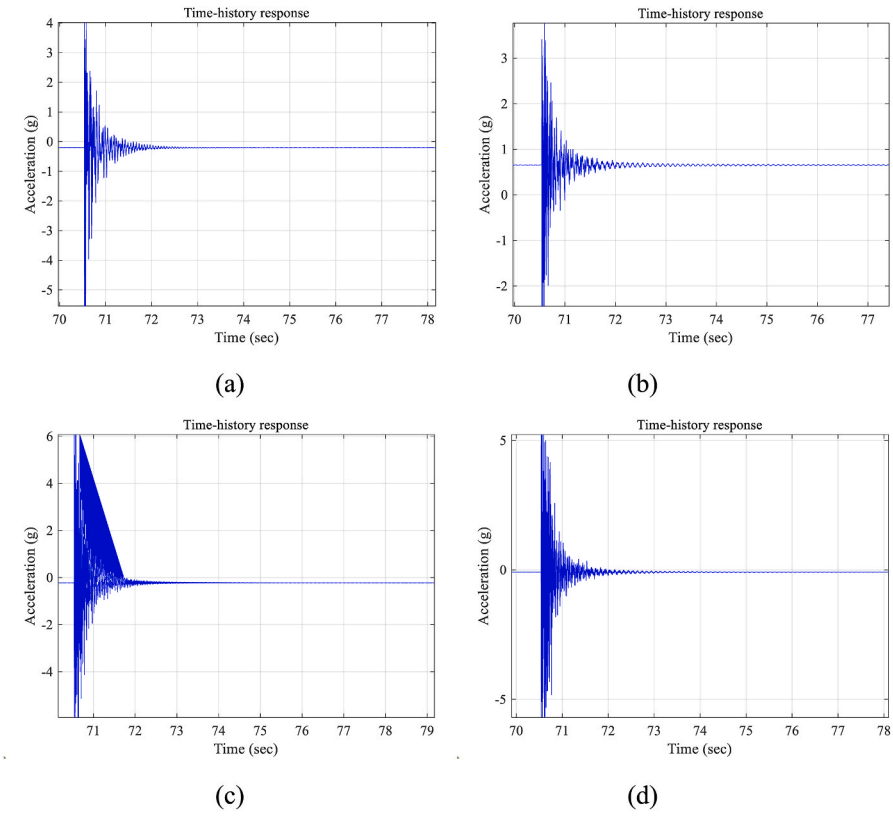

Fig. 17. Vibration measurements in multiple-damage condition. (a) Sensor #14X; (b) sensor #14Y; (c) sensor #10X; (d) sensor #10Y.

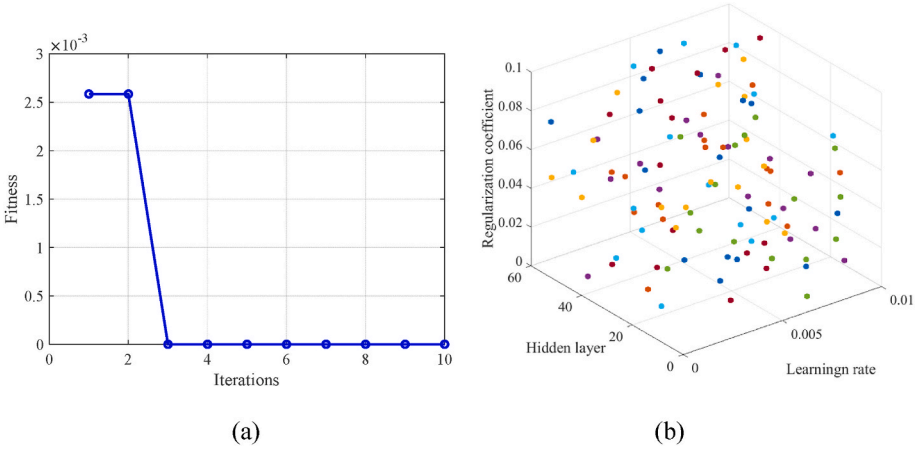

Fig. 18. The PSO optimization results. (a) The changes of the fitness function; (b) particle distribution.

Table 5
Parameters of the ensemble model.

Parameter	Value
Batch_size (size of the batch)	100
Filters (number of convolution cores)	8
Epochs (iteration number)	600
The channel of covn_1	16
The channel of covn_2	32
Optimizer	Adam
best_hd (number of hidden layers)	37
best_lr (learning rate)	0.0053
best_l2 (regularization coefficient)	0.03

vibration dataset with a time window of 0.08 s to generate a total of 1000 data samples, of which 80% were used as training set and the remaining 20% was used for performance testing and verification.

3.2. Feature extraction

In the data preprocessing, after normalizing and tiling the raw vibration data, the CNN was used to extract a 400*1*1 feature matrix from the vibration data, where 400 represents the number of features of each sample. The CNN parameter setting is listed in Table 2, and Fig. 9 depicts the visualization results of the feature extraction of the conv_2 convolution layer.

Meanwhile, the SENet attention calculates the weight of each feature channel of the conv_2 convolution layer, as described in Fig. 3. By

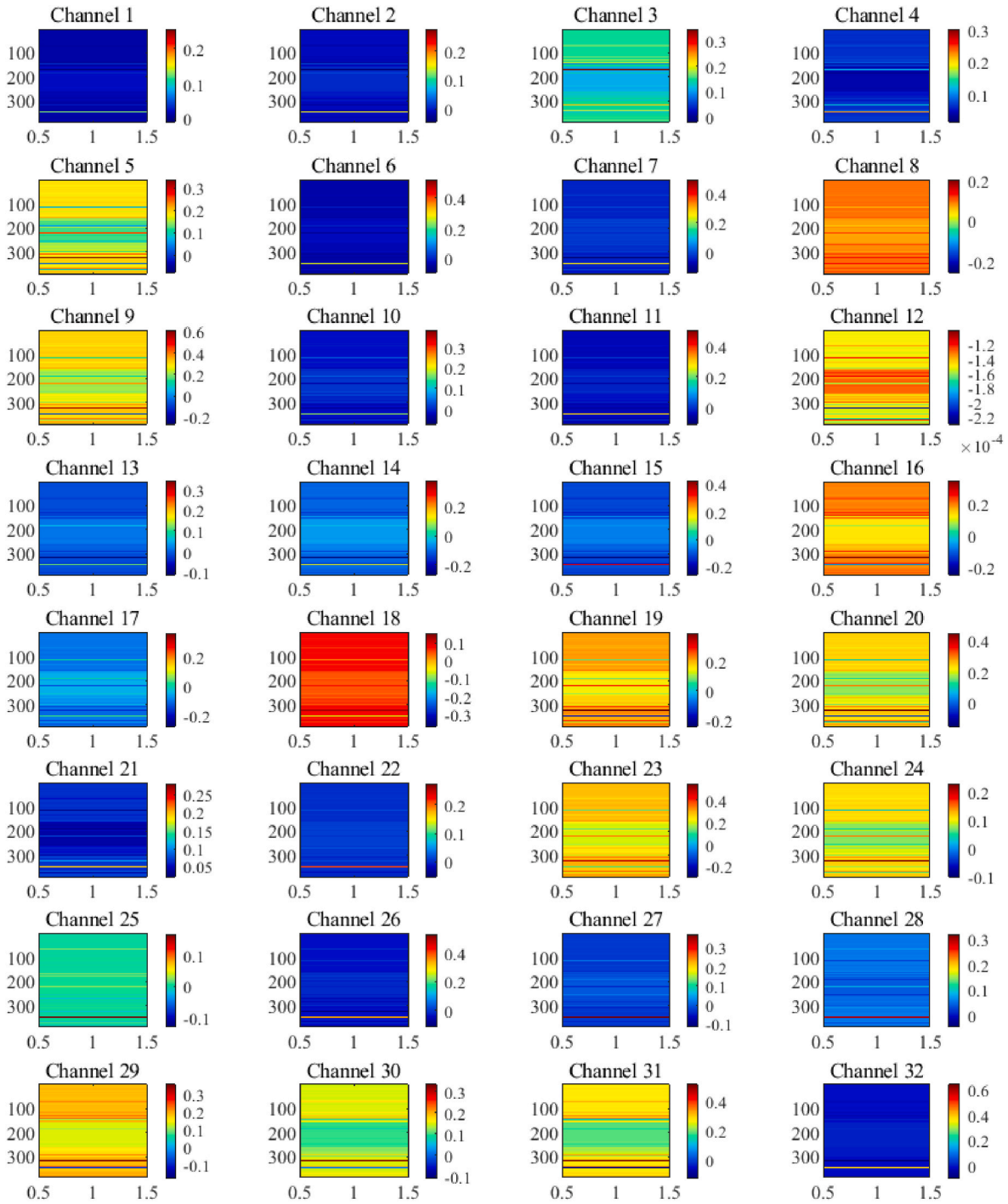

Fig. 19. The feature map of the output of the conv_2.

normalizing the weight values, the weight information of each channel of the conv_2 convolution layer is shown in Fig. 10.

To clearly present the weight information generated by the attention mechanism, the weight values are shown in Fig. 11.

As can be seen in Fig. 11, the weight values vary in different feature channel, which means the importance of different features is completely different. For example, the weight value is 1 for the feature channel 3, which indicates that this feature is the most important/informatic one. On the contrary, the weight value is 0.05 for the feature channel 33, and as a result, this feature is regarded as useless one and will be eliminated at the multiplication layer. By checking Fig. 11, one can note that the informatic features can be selected by the SENet attention using the weight values.

Subsequently, the obtained weights were multiplied with the output of the CNN layer (see Fig. 3) at the multiplication layer to determine the final features. This operation can be seen as a modulation mechanism, which adjusts the characteristics of different channels to focus on the critical information about the structure vibration measurements.

3.3. *BiLSTM optimization*

In the process of hyper-parameter optimization for the BiLSTM, the PSO was used to optimize the learning rate, the number of hidden layers and the regularization coefficient of the BiLSTM. The Mean Squared

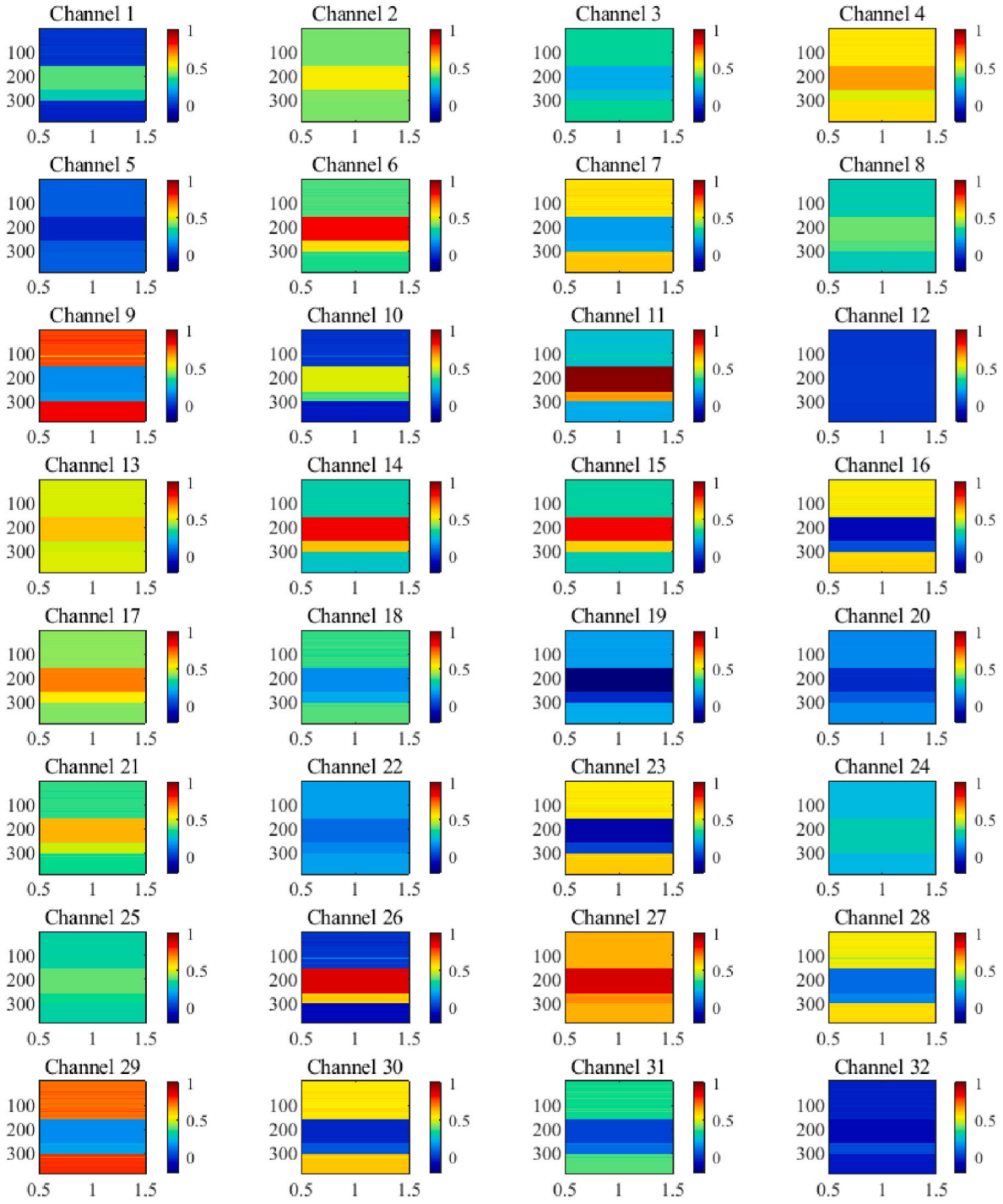

Fig. 20. The calculated weight by the SENet attention mechanism.

Error (MSE) was taken as the optimization evaluation metric. The optimization results are in Fig. 12.

It can be seen from Fig. 12 that the fitness function tends to be stable after 10 iterations, which means that the expected optimal hyper-parameters are obtained (i.e., subject to a set MSE constrain). The final optimized hyper-parameters were determined after the PSO optimization, i.e., the number of hidden layers (best_hd) = 15, the learning rate (best_lr) = 0.006, and the regularization coefficient (best_l2) = 0.0001.

3.4. Damage pattern identification

The extracted features were input into the BiLSTM model for damage pattern identification. Fig. 13 shows the identification results. It can be observed that the identification accuracy of the damage patterns for the training set achieves 100%; for the testing set, only four samples are misidentified, and the overall identification accuracy is 98.65%. The identification results in Fig. 13 indicates satisfactory performance of the proposed ensemble model for the damage pattern identification of the jacket platform.

To highlight the performance of the proposed model, the confusion matrix is provided for the damage pattern identification in Fig. 14. The

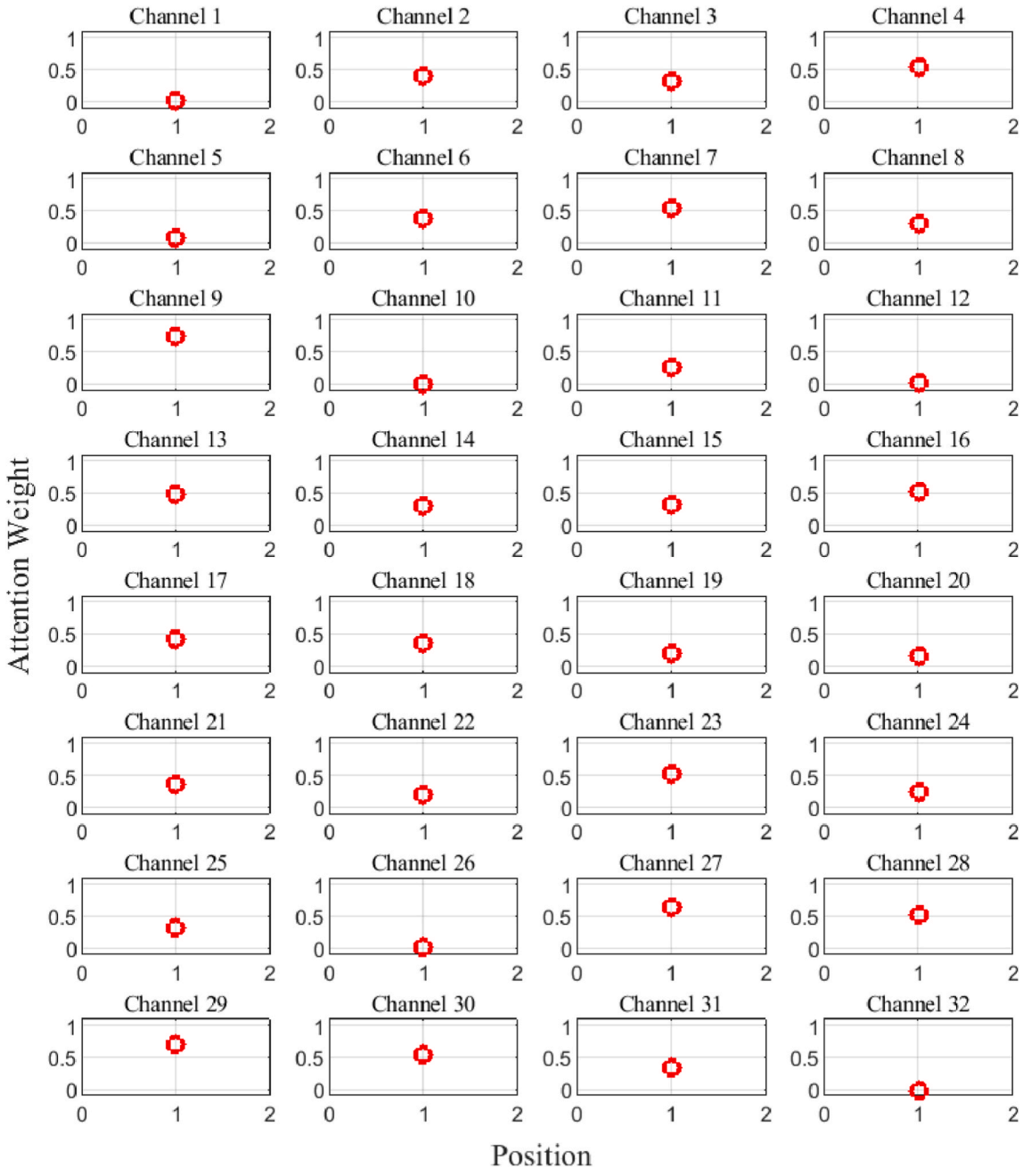

Fig. 21. The weight information of the first feature in different channels.

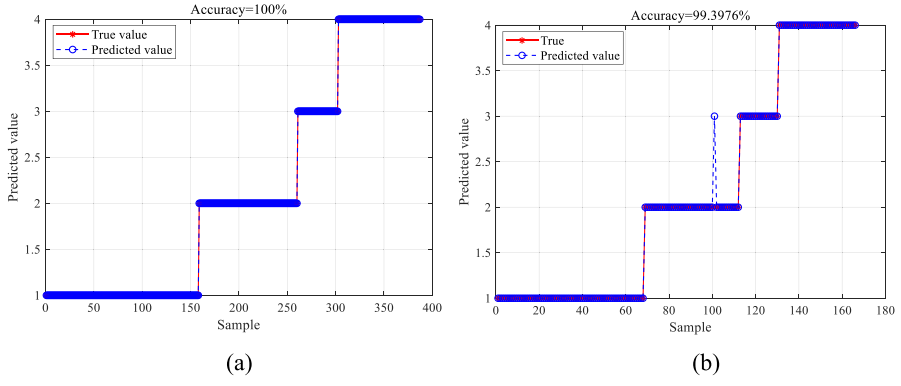

Fig. 22. The accuracy for training and validation. (a) Training set; (b) testing set.

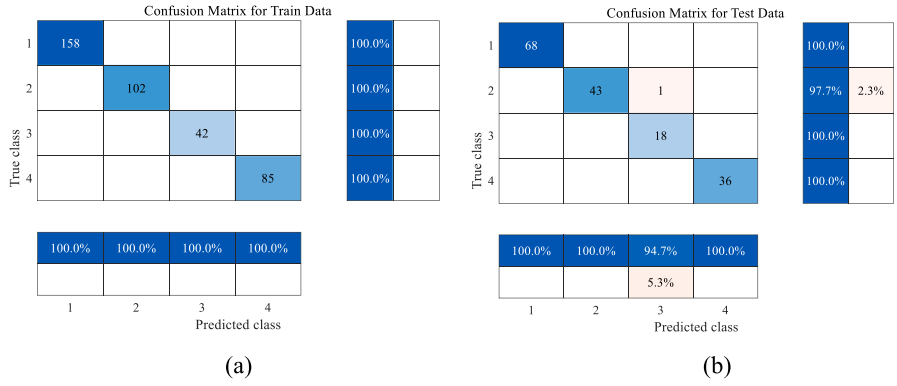

Fig. 23. The confusion matrix for training and validation. (a) Training set; (b) testing set.

Table 6
Comparison results of different models.

Model	*Accuracy*	*Precision*	*Recall*	*F*1 score
CNN	0.7892	0.8167	0.7635	0.7892
BiLSTM	0.9759	0.9819	0.9755	0.9787
CNN-BiLSTM-Attention	0.9940	0.9867	0.9943	0.9905

matrix presents the classification results of the four health conditions of the FE simulations. The detailed classification information, including the number of true cases, true negative cases, false positive cases, and false negative cases, is counted in the confusion matrix. The columns of the confusion matrix calculate the *Precision* metric, while the rows of the confusion matrix calculate the *Recall* metric. By analyzing the confusion matrix, one can observe that both the *Precision* and *Recall* reach 100% for each health condition in the training set. In the testing set, both the *Precision* and *Recall* exceed 95%. These observations demonstrate that the proposed ensemble model is able to solve the damage pattern identification problem for the jacket platform.

Furthermore, the performance of the proposed model was compared with the CNN model and the BiLSTM model. Table 3 lists the comparison results in terms of the four metrics of the *Accuracy*, *Precision*, *Recall* and *F*1 score. As can be seen that the single use of the CNN model produces the worst identification performance with unacceptable metric values. The single use of the BiLSTM model produces acceptable damage identification performance, and each metric in the table reaches a high value about 0.93. However, the proposed model generates obvious higher metric values (0.98) than these of the BiLSTM model, i.e., 5.38% improvement over the BiLSTM model. Considering a huge market (more than USD 20 billion per year) of operation and maintenance for wind farms, an improvement of 5.38% accuracy in the damage identification will prevent significant loss. As a result, the proposed ensemble model has great practical importance.

4. Experimental evaluation

4.1. Jacket structure prototype

A prototype of the jacket structure was developed to evaluate the proposed model in this work. The geometrical dimensions of the prototype were the same as the FE model, as shown in Fig. 15. The jacket model was welded with Q235 round tubes, and its material properties included an elastic modulus of 206 GPa, a mass density of 7850 kg/m^3, and a Poisson ratio of 0.3. The bottom of the jacket platform was fixed to a base made of steel plates, and a 12 kg steel plate was attached to the top of the structure to simulate the load of the turbine. The prototype consisted of four floors using 46 elements, including 12 main braces, 16 transverse braces and 2 diagonal braces. There were 25 nodes in the prototype, each node had 6 degrees of freedom, and the prototype had 150 degrees of freedom in total. From the bottom to the top, the width between each floor was 0.39, 0.30, 0.22 and 0.13 m, while the vertical height of each level was 0.65 m. The inner and outer diameters of the main brace were respectively 26.5 mm and 32 mm. The inner and outer diameters of the transverse and diagonal braces were respectively 13.6 mm and 16 mm.

In the experimental evaluation, the cross-sectional area of the element of interest was reduced to simulate the structural damage. Four health conditions were set up in the study, including the normal condition, single-damage condition, double-damage condition, and multiple-damage condition. The details of the four health conditions of the prototype are illustrated in Table 4 and the schematic diagram of the four conditions is explained in Fig. 16.

In the experiment, to comprehensively capture the vibration characteristics of the structure, accelerometers were installed along both the X and Y axes at each node. There were 32 sensors in total, installed on node no. 5, 6, 7, 8, 9, 10, 11, 12, 13, 14, 15, and 16. All sensors were connected to a signal acquisition instrument (CRONOS PL 64-DCB8) to collect and store vibration signals of the prototype in real time at a sampling frequency of 1000 Hz. During the test, a hammer was used to apply a impact load to the top plate from the X and Y directions to simulate the wind and wave loads of the jacket structure. Taking sensors #14X, #14Y, #10X, and #10Y as an example, the vibration signals in the multiple-damage condition are shown in Fig. 17.

As can be seen from Fig. 17, each sensor presents a tendency of rapid amplitude attenuation due to damping effect of the structure, which is similar to Fig. 8 in the FE simulations. A sliding window of 0.3 s was used to segment the vibration data to generate a total of 580 data samples, 80% of which were divided as the training set and 20% as testing set.

4.2. Parameters setting

The PSO was employed to optimize the learning rate, the number of hidden layers and the regularization coefficient of the BiLSTM model, and the MSE was taken as the optimization evaluation metric. Fig. 18 shows the fitness function and the particle distribution of the PSO. The PSO has reached convergence after 3 iterations in Fig. 18(a). The optimized hyper-parameters are listed in Table 5, which also shows the values of the CNN parameters.

4.3. Feature extraction

Fig. 19 shows the features extracted by the channel of covn_2 of the CNN, Fig. 20 presents the weight matrix of all channels for all features and Fig. 21 shows the weight values calculated by the SENet attention mechanism. It can be seen that in Fig. 21 the weight values of different channels vary significantly; however, in the original CNN model, the weight values of different channels are the same. As a result, the SENet

attention mechanism allows the CNN feature extraction to focus more on important features by dynamical weights.

4.4. Damage pattern identification

After the feature extraction, the BiLSTM model was used to recognize the damage patterns of the prototype. Fig. 22 gives the identification results for each sample in the training set and testing set. Meanwhile, Fig. 23 shows the confusion matrix during training and testing processes. It is worth noting that in the training set, the model achieves accurate prediction for each sample, and the overall accuracy reaches 100%. Although in the testing set a few samples are misidentified, the overall accuracy is still as high as 99.39 %. The experimental results demonstrate that the proposed ensemble model has strong generalization ability in the damage pattern identification of the jacket platform. The feasibility of the proposed method in practical application has been verified in both the simulation and experimental evaluations.

To highlight the effectiveness of the ensemble model, Table 6 presents the comparison of the recognition results of the CNN, BiLSTM and CNN-BiLSTM-Attention models. It can be seen from the table that the ensemble model has the best performance among these three methods by an improvement of 25.32% over the CNN and an improvement of 2.06% over the BiLSTM, respectively. The reason is probably that the ensemble model aggregates the CNN and BiLSTM into a strong framework using appropriate strategies (i.e. integrating the attention mechanism and the PSO optimization). As a result, the ensemble model produces better capacity and ability than the single use of each technique in the structural damage identification.

In summary, the proposed ensemble deep learning model has addressed the research gap in data-driven offshore structure monitoring by overcoming the challenge in the damage feature selection and damage pattern recognition.

5. Conclusions

This paper introduces a novel approach for structural health monitoring of offshore jacket platforms through the development of an ensemble deep learning model. This new model distinguishes itself by adeptly amalgamating different neural network architectures to harness the strengths of each one, thereby enabling the ensemble to prioritize critical information of the damages and effectively identify the damage patterns. The synergistic strategy significantly enhances the accuracy and reliability of proposed ensemble model for structural health monitoring.

The effectiveness of the ensemble model is corroborated by simulations using a FE model and experiments using a jacket platform. The identification accuracy of the FE model damages is around 98% and the accuracy in the experimental tests is around 99%, which demonstrates high adaptability to various data sources and good reliability to different damage patterns of the proposed method. Hence, the proposed ensemble model represents new methodology and perspective for damage detection of offshore jacket platforms, which provides essential technical support for structural health monitoring.

However, the performance of the current ensemble model significantly depends on the quality and diversity of the training data; we are planning to employ data augmentation techniques, transfer learning techniques and new datasets to improve the generalizability of the proposed model. Additionally, we acknowledge the limitations associated with the model in terms of real-time monitoring and computational resource demands. Future efforts will concentrate on refining and simplifying the model to meet real-time monitoring needs while reducing reliance on computational resources.

CRediT authorship contribution statement

Mengmeng Wang: Writing – original draft, Investigation, Formal analysis, Data curation. **Atilla Incecik:** Writing – review & editing, Supervision, Resources, Project administration, Funding acquisition. **Zhe Tian:** Validation, Methodology, Formal analysis. **Mingyang Zhang:** Software, Methodology, Investigation, Data curation. **Pentti Kujala:** Writing – review & editing, Supervision, Resources, Project administration, Funding acquisition. **Munish Gupta:** Software, Resources, Methodology, Investigation. **Grzegorz Krolczyk:** Visualization, Validation, Software, Resources, Project administration. **Zhixiong Li:** Writing – original draft, Supervision, Resources, Methodology, Conceptualization.

Declaration of competing interest

The authors declare that they have no known competing financial interests or personal relationships that could have appeared to influence the work reported in this paper.

Data availability

Data will be made available on request.

Acknowledgements

This research is supported by the National Natural Science Foundation of China under the grant no. 52271296 and 51979261, and the Opole University of Technology as part of the GRAS project no. 270/23. The research leading to these results has received funding from the Norwegian Financial Mechanism 2014–2021 under Project Contract No 2020/37/K/ST8/02748.

References

Aeran, A., Acosta, R., Siriwardane, S.C., Starke, P., Mikkelsen, O., Langen, I., Walther, F., 2020. A nonlinear fatigue damage model: comparison with experimental damage evolution of S355 (SAE 1020) structural steel and application to offshore jacket structures. Int. J. Fatig. 135, 105568 https://doi.org/10.1016/j.ijfatigue.2020.105568.

Ahmadian, V., Beheshti Aval, S.B., Noori, M., Wang, T., Altabey, W.A., 2024. Comparative study of a newly proposed machine learning classification to detect damage occurrence in structures. Eng. Appl. Artif. Intell. 127, 107226 https://doi.org/10.1016/j.engappai.2023.107226.

Aravind Britto, K.R., Srinivasan, S., Mathivanan, S.K., Venkatesan, M., Benjula Anbu Malar, M.B., Mallik, S., Qin, H., 2023. A multi-dimensional hybrid CNN-BiLSTM framework for epileptic seizure detection using electroencephalogram signal scrutiny. Systems and Soft Computing 5, 200062. https://doi.org/10.1016/j.sasc.2023.200062.

Asgarian, B., Aghaeidoost, V., Shokrgozar, H.R., 2016. Damage detection of jacket type offshore platforms using rate of signal energy using wavelet packet transform. Mar. Struct. 45, 1–21. https://doi.org/10.1016/j.marstruc.2015.10.003.

Augustyn, D., Smolka, U., Tygesen, U.T., Ulriksen, M.D., Sørensen, J.D., 2020. Data-driven model updating of an offshore wind jacket substructure. Appl. Ocean Res. 104, 102366 https://doi.org/10.1016/j.apor.2020.102366.

Balu, A., Sarkar, S., Ganapathysubramanian, B., Krishnamurthy, A., 2022. Physics-aware machine learning surrogates for real-time manufacturing digital twin. Manufacturing Letters 34, 71–74. https://doi.org/10.1016/j.mfglet.2022.08.013.

Bao, X., Fan, T., Shi, C., Yang, G., 2021. One-dimensional convolutional neural network for damage detection of jacket-type offshore platforms. Ocean. Eng. 219, 108293 https://doi.org/10.1016/j.oceaneng.2020.108293.

Cattaneo, L., Macchi, M., 2019. A digital twin proof of concept to support machine prognostics with low availability of run-to-failure data. IFAC-PapersOnLine 52, 37–42. https://doi.org/10.1016/j.ifacol.2019.10.016.

Chakraborty, S., Adhikari, S., 2021. Machine learning based digital twin for dynamical systems with multiple time-scales. Comput. Struct. 243, 106410 https://doi.org/10.1016/j.compstruc.2020.106410.

Chen, Y., Zhang, Q., Wang, X., Yao, Z., 2022. Interactions between a cavitation bubble and solidification front under the effects of ultrasound: experiments and lattice Boltzmann modeling. Ultrason. Sonochem. 91, 106221 https://doi.org/10.1016/j.ultsonch.2022.106221.

Dou, P., Zou, L., Wu, T., Yu, M., Reddyhoff, T., Peng, Z., 2022. Simultaneous measurement of thickness and sound velocity of porous coatings based on the ultrasonic complex reflection coefficient. NDT E Int. 131, 102683 https://doi.org/10.1016/j.ndteint.2022.102683.

Ebrahimian, H., Astroza, R., Conte, J.P., de Callafon, R.A., 2017. Nonlinear finite element model updating for damage identification of civil structures using batch Bayesian estimation. Mechanical Systems and Signal Processing, Recent advances in nonlinear system identification 84, 194–222. https://doi.org/10.1016/j.ymssp.2016.02.002.

Fathi, A., Esfandiari, A., Fadavie, M., Mojtahedi, A., 2020. Damage detection in an offshore platform using incomplete noisy FRF data by a novel Bayesian model updating method. Ocean. Eng. 217, 108023 https://doi.org/10.1016/j.oceaneng.2020.108023.

Ghiasi, A., Moghaddam, M.K., Ng, C.-T., Sheikh, A.H., Shi, J.Q., 2022. Damage classification of in-service steel railway bridges using a novel vibration-based convolutional neural network. Eng. Struct. 264, 114474 https://doi.org/10.1016/j.engstruct.2022.114474.

Guo, H., Shi, Y., Pan, F., Zheng, S., Chai, X., Yang, Y., Jiang, H., Wang, X., Li, L., Xiu, Z., Wang, J., Lu, W., 2023. Tough, stretchable dual-network liquid metal-based hydrogel toward high-performance intelligent on-off electromagnetic interference shielding, human motion detection and self-powered application. Nano Energy 114, 108678. https://doi.org/10.1016/j.nanoen.2023.108678.

Huang, J., Li, Y., Yuan, G., Liu, Q., Zuo, T., Xu, G., Lv, J., Ding, X., Hong, Y., Luo, L., Tan, X., Chen, J., Wu, Y., 2022. Corrosion and microstructure evolution of He+ plasma irradiated tungsten PFMs. Fusion Eng. Des. 184, 113279 https://doi.org/10.1016/j.fusengdes.2022.113279.

Huang, Q., Gardoni, P., Hurlebaus, S., 2012. A probabilistic damage detection approach using vibration-based nondestructive testing. Struct. Saf. 38, 11–21. https://doi.org/10.1016/j.strusafe.2012.01.004.

Jamshidi, M., El-Badry, M., 2023. Structural damage severity classification from time-frequency acceleration data using convolutional neural networks. Structures 54, 236–253. https://doi.org/10.1016/j.istruc.2023.05.009.

Karthika, S., Rathika, P., 2024. An adaptive data compression technique based on optimal thresholding using multi-objective PSO algorithm for power system data Image 1. Appl. Soft Comput. 150, 111028 https://doi.org/10.1016/j.asoc.2023.111028.

Khodaparast, H.H., Mottershead, J.E., Badcock, K.J., 2011. Interval model updating with irreducible uncertainty using the Kriging predictor. Mech. Syst. Signal Process. 25, 1204–1226. https://doi.org/10.1016/j.ymssp.2010.10.009.

Kilic, F., Korkmaz, M., Er, O., Altin, C., 2023. A CNN-based novel approach for classification of sacral hiatus with GAN-powered tabular data set. Elektronika Ir Elektrotechnika 29 (2), 44–53. https://doi.org/10.5755/j02.eie.33852.

Kouchaki, M., Salkhordeh, M., Mashayekhi, M., Mirtaheri, M., Amanollah, H., 2023. Damage detection in power transmission towers using machine learning algorithms. Structures 56, 104980. https://doi.org/10.1016/j.istruc.2023.104980.

Liu, K., Yan, R.-J., Guedes Soares, C., 2018. Damage identification in offshore jacket structures based on modal flexibility. Ocean. Eng. 170, 171–185. https://doi.org/10.1016/j.oceaneng.2018.10.014.

Lu, C., Li, L., Liu, Z., Xu, C., Xin, M., Fu, G., Wang, T., Wang, X., 2022. Location and corrosion detection of tower grounding conductors based on electromagnetic measurement. Measurement 199, 111469. https://doi.org/10.1016/j.measurement.2022.111469.

Meng, J., Zhen, Y., Zhang, K., Zhang, J., Zhao, H., Li, J., 2023. Quantitative detection and evaluation of Rayleigh ultrasonic wave for fatigue crack on turbine blade surface. Appl. Acoust. 211, 109558 https://doi.org/10.1016/j.apacoust.2023.109558.

Mojtahedi, A., Hokmabady, H., Yaghubzadeh, A., Mohammadyzadeh, S., 2020. An improved model reduction-modal based method for model updating and health monitoring of an offshore jacket-type platform. Ocean. Eng. 209, 107495 https://doi.org/10.1016/j.oceaneng.2020.107495.

Mojtahedi, A., Lotfollahi Yaghin, M.A., Hassanzadeh, Y., Ettefagh, M.M., Aminfar, M.H., Aghdam, A.B., 2011. Developing a robust SHM method for offshore jacket platform using model updating and fuzzy logic system. Appl. Ocean Res. 33, 398–411. https://doi.org/10.1016/j.apor.2011.05.001.

Moradzadeh, A., Teimourzadeh, H., Mohammadi-Ivatloo, B., Pourhossein, K., 2022. Hybrid CNN-LSTM approaches for identification of type and locations of transmission line faults. Int. J. Electr. Power Energy Syst. 135, 107563 https://doi.org/10.1016/j.ijepes.2021.107563.

Mousavi, Z., Varahram, S., Mohammad Ettefagh, M., Sadeghi, M.H., 2023. Dictionary learning-based damage detection under varying environmental conditions using only vibration responses of numerical model and real intact State: verification on an experimental offshore jacket model. Mech. Syst. Signal Process. 182, 109567 https://doi.org/10.1016/j.ymssp.2022.109567.

Nguyen, H.L., Woon, Y.K., Ng, W.K., 2015. A survey on data stream clustering and classification. Knowl. Inf. Syst. 45, 535–569. https://doi.org/10.1007/s10115-014-0808-1.

Ni, Q.-Q., Hong, J., Xu, P., Xu, Z., Khvostunkov, K., Xia, H., 2021. Damage detection of CFRP composites by electromagnetic wave nondestructive testing (EMW-NDT). Compos. Sci. Technol. 210, 108839 https://doi.org/10.1016/j.compscitech.2021.108839.

Pan, S., Yang, B., Wang, S., Guo, Z., Wang, L., Liu, J., Wu, S., 2023. Oil well production prediction based on CNN-LSTM model with self-attention mechanism. Energy 284, 128701. https://doi.org/10.1016/j.energy.2023.128701.

Puruncajas, B., Vidal, Y., Tutivén, C., 2020. Vibration-response-only structural health monitoring for offshore wind turbine jacket foundations via convolutional neural networks. Sensors 20, 3429. https://doi.org/10.3390/s20123429.

Qin, F., Li, B., Chen, L., Shang, Z., Zhang, Z., Huang, Y., Wang, W., Zheng, Y., 2023. Interaction analysis of different defects with laser ultrasonic sound waves and defect characterization. Opt Laser. Technol. 157, 108630 https://doi.org/10.1016/j.optlastec.2022.108630.

Richmond, M., Smolka, U., Kolios, A., 2020. Feasibility for damage identification in offshore wind jacket structures through monitoring of global structural dynamics. Energies 13, 5791. https://doi.org/10.3390/en13215791.

Shiradhonkar, S.R., Shrikhande, M., 2011. Seismic damage detection in a building frame via finite element model updating. Comput. Struct. 89, 2425–2438. https://doi.org/10.1016/j.compstruc.2011.06.006.

Serkan, K., Onur, A., Osama, A., Turker, I., Moncef, G., Daniel, I., 2021. 1D convolutional neural networks and applications: a survey. Mech. Syst. Signal Process. 151, 107398 https://doi.org/10.1016/j.ymssp.2020.107398.

Utaminingrum, F., Alqadri, A.M., Somawirata, I.K., Karim, C., Septiarini, A., Lin, C.-Y., Shih, T.K., 2023. Feature selection of gray-level Cooccurrence matrix using genetic algorithm with Extreme learning machine classification for early detection of Pole roads. Results in Engineering 20, 101437. https://doi.org/10.1016/j.rineng.2023.101437.

Wang, M., Incecik, A., Feng, S., Gupta, M.K., Królczyk, G., Li, Z., 2023. Damage identification of offshore jacket platforms in a digital twin framework considering optimal sensor placement. Reliab. Eng. Syst. Saf. 237, 109336 https://doi.org/10.1016/j.ress.2023.109336.

Wang, M., Leng, J., Feng, S., Li, Z., Incecik, A., 2022. Precisely modeling offshore jacket structures considering model parameters uncertainty using Bayesian updating. Ocean. Eng. 258, 111410 https://doi.org/10.1016/j.oceaneng.2022.111410.

Wang, Y., Zhang, Z., Wang, Youyun, You, L., Wei, G., 2023. Modeling and structural optimization design of switched reluctance motor based on fusing attention mechanism and CNN-BiLSTM. Alex. Eng. J. 80, 229–240. https://doi.org/10.1016/j.aej.2023.08.039.

Xu, M., Guo, J., Wang, S., Li, J., Hao, H., 2021. Structural damage identification with limited modal measurements and ultra-sparse Bayesian regression. Struct. Control Health Monit. 28, e2729 https://doi.org/10.1002/stc.2729.

Zahs, V., Anders, K., Kohns, J., Stark, A., Höfle, B., 2023. Classification of structural building damage grades from multi-temporal photogrammetric point clouds using a machine learning model trained on virtual laser scanning data. Int. J. Appl. Earth Obs. Geoinf. 122, 103406 https://doi.org/10.1016/j.jag.2023.103406.

Zhang, D., Du, J., Yuan, Z., Yu, S., Li, H., 2023. Motion characteristics of large arrays of modularized floating bodies with hinge connections. Phys. Fluids 35, 077107. https://doi.org/10.1063/5.0153317.

Zhang, D., Yuan, Z.-M., Du, J., Li, H., 2022. Hydrodynamic modelling of large arrays of modularized floating structures with independent oscillations. Appl. Ocean Res. 129, 103371 https://doi.org/10.1016/j.apor.2022.103371.

Zhang, F., Luo, L., Li, J., Peng, J., Zhang, Y., Gao, X., 2023. Ultrasonic adaptive plane wave high-resolution imaging based on convolutional neural network. NDT E Int. 138, 102891 https://doi.org/10.1016/j.ndteint.2023.102891.

Zhang, M., Chen, R., Zheng, L., Yao, J., Liu, F., Chen, Y., 2022. Electromagnetic ultrasonic signal processing and imaging for debonding detection of bonded structures. Measurement 205, 112106. https://doi.org/10.1016/j.measurement.2022.112106.

Zhang, M., Tsoulakos, N., Kujala, P., Hirdaris, S., 2024. A deep learning method for the prediction of ship fuel consumption in real operational conditions. Eng. Appl. Artif. Intell. 130, 107425 https://doi.org/10.1016/j.engappai.2023.107425.